A High Order Accurate and Robust Fiber Tractography with Diffusion Tensor Imaging

Y. Lu[1], J. Qi[1], D. Wang[1], A. Anderson[2], J. Gore[2], and Z. Ding[2]

[1]Radiology Department, The First Affiliated Hospital of Nanjing Medical University, Nanjing, Jiangsu Province, China, People's Republic of, [2]Vanderbilt University Institute of Imaging Science, Nashville, TN, United States

Introduction

Diffusion tensor imaging (DTI) based fiber tractography is a promising technique for characterizing fiber pathways *in vivo.* A main concern of this technique is the accuracy and robustness in the presence of noise and partial volume averaging (PVA). Although many algorithms have been proposed to address this [1], few of them are accurate and robust simultaneously with these artifacts. In this study, a novel method based on multi-step numerical method and Bayes decision rule is proposed. Experiments show the proposed method has both high order accuracy and robustness in fiber tracking with noise and PVA.

Methods

The evolution of a fiber tract trajectory can be described by ordinary differential equation (ODE) with an initial condition [2]:

$$\frac{d\,\boldsymbol{r}(s)}{ds} = \mu(s), \quad \boldsymbol{r}(0) = \boldsymbol{r}_0$$

Where $\boldsymbol{r}(s)$ is the fiber position vector at arc length s, $\boldsymbol{\mu}(s)$ the major eigenvector at s, $\boldsymbol{r}_0$ the initial position.

In contrast to other single-step methods reported (e.g., Euler or Runge-Kutta method [2]), the proposed solution of the ODE in this study is a specially designed multi-step method, referred to as Bayesian Regularized Adam-Bashforth (BRAB) method, i.e.:

(1) It uses Adam-Bashforth method [3] to calculate the fiber position at each step:

$$r(s_{n+1}) = r(s_n) + \Delta s(55\mu(s_n) - 59\mu(s_{n-1}) + 37\mu(s_{n-2}) - 9\mu(s_{n-3}))$$

Where Δs is the step size.

Compared to the Euler method's 1st order accuracy, the Adam-Bashforth method has 4th-order accuracy. Additionally, since the Adam-Bashforth method fits previous points as a polynomial to predict the next point, the method can enable fiber propagation robust to the effect of PVA.

(2) It uses a Bayesian framework to regularize the major eigenvector at each step. The Bayes decision in tensor regularization is to determine the value of $\boldsymbol{\mu}$ that maximizes the *a posteriori* (MAP) probability $P(\boldsymbol{\mu}_j|\boldsymbol{x})$, which is the product of the conditional probability density $p(\boldsymbol{x}|\boldsymbol{\mu}_j)$ and the *a priori* probability $P(\boldsymbol{\mu}_j)$, i.e.:

$$\boldsymbol{\mu} = argmax(P(\boldsymbol{\mu}_j \mid \boldsymbol{x})) = argmax(p(\boldsymbol{x} \mid \boldsymbol{\mu}_j) \cdot P(\boldsymbol{\mu}_j), j = 1,2,...,n)$$

The noisy major eigenvectors are supposed to be normal distribution, i.e., $\boldsymbol{x} \sim N(\boldsymbol{\mu}_j, \sigma^2)$, $\boldsymbol{\mu}_j \sim N(\boldsymbol{m}, s^2)$. All related parameters, i.e. σ^2, $\mathbf{m}$, s^2, can be estimated from the measured data [4].

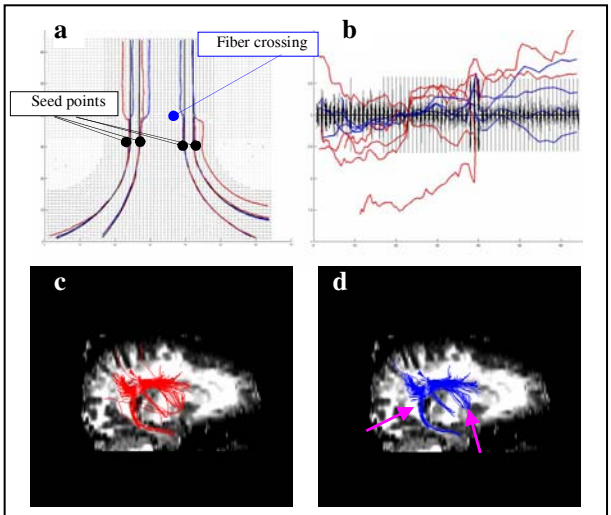

Figure 1. Results with synthetic and *in vivo* human data. **a**, Results with synthetic data by two methods. **b**, A detailed view of **a**; **c**. *In vivo* results by the Euler method; **d**, *In vivo* results by the BRAB method (black curve: true fibers; red curve: Euler method; blue curve: BRAB method; pink arrows: fiber difference between two methods).

The novelties of this proposed method are that it is not only 4th-order accurate, but also robust to noise, and particularly resists the effect of PVA.

Results

Synthetic and *in vivo* human DTI data were used to test the performance of this method. Synthetic data includes simulated straight and curved fiber tract trajectories with a fiber bundle crossing. Synthetic tensors were constructed to have a trace of $2.1*10^{-5}$ cm^2/s, and diffusion weighting was along six non-collinear directions with a b value of 1000 s/mm^2. Tensors for anisotropic regions were designed to be cylindrically symmetric ($\lambda_1 > \lambda_2 = \lambda_3$) with an identical eigenvalue contrast ($\Delta\lambda = \lambda_1 - \lambda_2 = 0.8*10^{-5}$ cm^2/s); tensors for isotropic regions and the fiber crossing area were isotropic ($\lambda_1 = \lambda_2 = \lambda_3$). The signal-to-noise ratio of this data set was 20, and the data size was 80*64*5 voxels. Human data were obtained on a 3T GE Signa MR scanner with data matrix of 256x256x30 and voxel size of 1x1x4 mm^3.

Figure 1(a) and 1(b) show the results with the synthetic data at selected seed points. Figure 1(b) is the different and detailed view of Figure 1(a). It can be shown that the proposed method can obtain smoother putative fibers with smaller deviation to the true tract trajectory than the Euler's method. Particularly in the region of fiber crossing, the proposed method can succeed in penetrating the area of fiber crossing while the Euler method fails. Figure 1(c) and 1(d) compare the putative fibers of these two methods in the superior longitudinal fasciculus of an *in vivo* human data set. In the region of high anisotropy, the fibers from both methods are similar, but in the low anisotropy area (indicating probable fiber intersection), they are different (shown as pink arrows in Figure 1(d)).

Discussion and conclusion

This study has demonstrated that the new approach has a superior performance of high order accuracy, noise reduction and PVA robustness in fiber tracking of diffusion tensor images. Further improvements of this method may include: 1. More complex multi-step scheme will be considered to improve the ability of PVA robustness of this method; 2. More general probability function instead of normal function will be considered that may reveal the true distribution of underlying fiber tract trajectories. 3. An anisotropic interpolation scheme instead of linear interpolation during fiber evolution will be employed to preserve the directional coherence and suppress undesirable artifacts induced in the process of interpolation; 4. The computation efficiency of this method will be improved as well in the future.

References

[1] Mori S et al., NMR in Biomedicine, 2002:15:468-480.
[2] Basser PJ et al., MRM 2000:44:625–632.
[3] Press WH et al., Numerical recipes in C, Cambridge University Press, 1988
[4] Lu Y et al., NeuroImage, 2006: 31:1061-1074.